# Alternative Pathway to Double-Core-Hole States

Iyas Ismail,[1,*] Anthony Ferté,[1] Francis Penent,[1] Renaud Guillemin,[1] Dawei Peng,[1,2] Tatiana Marchenko,[1] Oksana Travnikova,[1] Ludger Inhester,[3] Richard Taïeb,[1] Abhishek Verma,[1] Nicolas Velasquez,[1] Edwin Kukk,[1,4] Florian Trinter,[5,6] Dimitris Koulentianos,[7,3,8] Tommaso Mazza,[2] Thomas M. Baumann,[2] Daniel E. Rivas,[2] Yevheniy Ovcharenko,[2] Rebecca Boll,[2] Simon Dold,[2] Alberto De Fanis,[2] Markus Ilchen,[2] Michael Meyer,[2] Gildas Goldsztejn,[9] Kai Li,[7] Gilles Doumy,[7] Linda Young,[7,10] Giuseppe Sansone,[11] Reinhard Dörner,[5] Maria Novella Piancastelli,[1] Stéphane Carniato,[1] John D. Bozek,[12] Ralph Püttner,[13] and Marc Simon[1,†]

[1]*Sorbonne Université, CNRS, Laboratoire de Chimie Physique-Matière et Rayonnement, LCPMR, F-75005 Paris Cedex 05, France*

[2]*European XFEL, Holzkoppel 4, 22869 Schenefeld, Germany*

[3]*Center for Free-Electron Laser Science CFEL, Deutsches Elektronen-Synchrotron DESY, Notkestraße 85, 22607 Hamburg, Germany*

[4]*Department of Physics and Astronomy, University of Turku, FI-20014 Turku, Finland*

[5]*Institut für Kernphysik, Goethe-Universität Frankfurt, Max-von-Laue-Straße 1, 60438 Frankfurt am Main, Germany*

[6]*Molecular Physics, Fritz-Haber-Institut der Max-Planck-Gesellschaft, Faradayweg 4-6, 14195 Berlin, Germany*

[7]*Chemical Sciences and Engineering Division, Argonne National Laboratory, 9700 South Cass Avenue, Argonne, Illinois 60439, USA*

[8]*Department of Physics, Universität Hamburg, Luruper Chaussee 149, 22761 Hamburg, Germany*

[9]*Université Paris-Saclay, Institut des Sciences Moléculaires d'Orsay ISMO, UMR CNRS 8214, F-91405 Orsay, France*

[10]*Department of Physics and James Franck Institute, The University of Chicago, Chicago, Illinois, USA*

[11]*Institute of Physics, University of Freiburg, Hermann-Herder-Straße 3, 79104 Freiburg, Germany*

[12]*Synchrotron SOLEIL, L'Orme des Merisiers, Saint-Aubin, F-91192 Gif-sur-Yvette Cedex, France*

[13]*Fachbereich Physik, Freie Universität Berlin, Arnimallee 14D-14195 Berlin, Germany*

(Received 16 August 2023; revised 23 October 2023; accepted 1 November 2023; published 20 December 2023)

Excited double-core-hole states of isolated water molecules resulting from the sequential absorption of two x-ray photons have been investigated. These states are formed through an alternative pathway, where the initial step of core ionization is accompanied by the shake-up of a valence electron, leading to the same final states as in the core-ionization followed by core-excitation pathway. The capability of the x-ray free-electron laser to deliver very intense, very short, and tunable light pulses is fully exploited to identify the two different pathways.

DOI: 10.1103/PhysRevLett.131.253201

X-ray free-electron lasers (XFELs) have the unique ability to produce a very high density of x-ray photons within an ultrashort pulse duration. This allows for the interaction of an atom or molecule with multiple photons, resulting in what is called sequential excitation or sequential ionization. The high intensity of the photon beam in combination with the short pulse duration can be used to produce, for example, electronic states such as double-core-hole (DCH) states with holes in the K shell, either as dication ($K^{-2}$) or as monocation with one additional electron in the valence shell ($K^{-2}V$) [1–3].

The lifetimes of the double-core-hole states are much shorter than those of single-core-hole (SCH) states [4–6]. This is the reason why the DCH states can be used as a femtosecond probe, allowing, for instance, a breakthrough to earlier stage (1 fs) of the interaction of water with x rays [7]. Moreover, DCH states are of great interest because they are much more sensitive to the chemical environment compared to the SCH ionic states [1,8–10]. Studying DCH states is particularly relevant for the radiation damage in experiments at high-intensity x-ray radiation, because they lead to temporary reduced x-ray absorption cross sections. This phenomenon termed x-ray induced transparency [11] or frustrated absorption [12] is particularly appealing for prospective single-molecule diffractive imaging experiments [13].

The signatures of these states with very short lifetimes, in the order of a femtosecond or below, are observable in the subsequent nonradiative relaxation processes, which in the case of monocations ($K^{-2}V$ states) can be viewed as resonant Auger decays of the produced DCH states. In these nonradiative decays, an electron from a higher energy level fills one of the two core holes, while another electron, a so-called hypersatellite Auger (HS) KVV1, is emitted into the continuum. The second core hole can be filled by a second step of Auger decay (KVV2). The HS Auger

 

electrons have a higher kinetic energy than those emitted in the Auger decay of SCH states. Measuring HS Auger electrons while tuning the photon energy allows us to map the monocationic $K^{-2}V$ resonances [3].

In this Letter, we report on various DCH excited states of $H_2O^+$ and $H_2O^{++}$ ions produced resonantly and selectively by sequential absorption of x-ray photons from the ground state (g.s.), via the excitation scheme O (g.s.) $\rightarrow$ O $1s^{-1} \rightarrow$ O $1s^{-2}$V or O $1s^{-2}$. In addition to these spectral features, where the excitation pathway is expected, we found additional resonance features with comparable intensity but at lower photon energies. Our calculations have revealed an alternative pathway to produce $H_2O^+$ and $H_2O^{++}$ DCH states with lower photon energies. The novel characteristics of this route are that it involves a shake-up state in the first step and a previously occupied and then vacated state reached in the second step. To the best of our knowledge, resonant nonlinear processes involving shake-up states as intermediate steps have not yet been discussed in the literature.

The identification of two different pathways leading to the same final state is made possible here by fully exploiting the characteristics of the light source, and namely its high intensity, time structure, and tunability at the same time.

A $K^{-2}V$ DCH state can be produced in two ways that depend on the photon energy (Fig. 1). In the "intuitive" pathway (denoted pathway A), as observed in Ref. [3], a first photon ionizes one $1s$ electron and a second photon excites the remaining $1s$ electron into an unoccupied orbital. For water, a photon energy around 616 eV is required for the O $1s^{-1} \rightarrow$ O $1s^{-2}$ $4a_1$ (LUMO) transition in the core-ionized $H_2O^+$ ion.

There is also an alternative pathway (called pathway B), in which the ionization with the first photon is accompanied by a shake-up of a valence electron. As shown in this Letter, in this case, the excitation in the second step is dominated by the promotion of the second $1s$ electron into the valence orbital depopulated by the shake-up process. In other words, in pathway B, a satellite of the O $1s$ ionization is the intermediate state. These states appear in an energy region of about 15–40 eV higher in energy than the O $1s$ main line [34] and allow for the population of the $K^{-2}V$ states in the second step with photons of lower energy (about 600 eV).

Figure 2(a) shows for $H_2O$ a 2D map obtained from the present measurement. In detail, we measured, using the time-of-flight (TOF) technique, electron spectra over a wide kinetic-energy range (several 100 eV) and changed the photon energy in energy steps of 1 eV. By plotting these electron spectra as a function of the photon energy ($x$ axis) we obtain 2D maps. In these maps, the kinetic energy of the electrons is given along the $y$ axis and the intensity is encoded by the different colors; see legend. In principle, the 2D maps display all processes that produce electrons, i.e.,

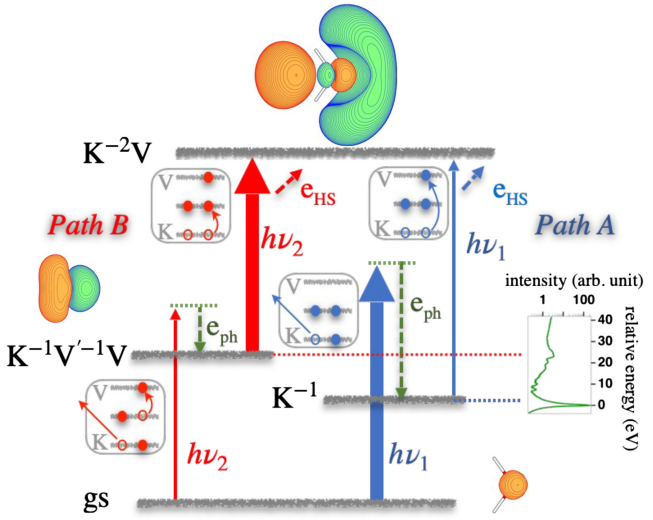


FIG. 1. Simplified schematic representation of the processes for the population of the $K^{-2}V$ DCH states by two-photon processes. Given are the ground state (g.s.), the $K^{-1}$ (right), the satellite $K^{-1}$ $V'^{-1}V$ (left), and the final $K^{-2}V$ states. Right: path A using two photons of energy $h\nu_1$: The first photon produces the $K^{-1}$ state and a second photon resonantly excites a $K^{-2}V$ state. Left: path B using two photons of energy $h\nu_2$: In the first step $K^{-1}$ $V'^{-1}V$ states are formed and in the second step $K^{-2}V$ states are populated. Note that $K^{-2}V$ states can be populated via two different photon energies, namely $h\nu_2 < h\nu_1$, since $E(K^{-1}\,V'^{-1}V) > E(K^{-1})$. Inset right: experimental O $1s$ photoelectron ($e_{ph}$) satellite spectrum of $H_2O$ using a photon energy of 616 eV and presenting the intensity on a logarithmic scale, it shows a $\approx 10^{-2}$ ratio of the peaks corresponding to $K^{-1}$ $V'^{-1}V$ and $K^{-1}$ states. The energy is given relative to the binding energy of the O $1s$ main line. We have illustrated the representative orbitals involved in path A and B, respectively; see also the Supplemental Material [14].

photoelectron spectra of neutral and ionized species as well as the Auger decay processes of the different SCH or DCH states. The process of interest can be displayed by selecting the corresponding photon-energy and the kinetic-energy intervals. In the present work, we study the DCH states by detecting the subsequent, i.e., first step HS Auger decay. For this purpose, the electron spectra are measured in the kinetic-energy range from 520 to 600 eV by using photon energies between 590 and 630 eV. For these measurements, the photon bandwidth is about 7 eV at full width at half maximum (FWHM). Moreover, the electron-energy resolution is estimated to be 0.7 eV. Figure 2 shows two diagonal structures that exhibit a linear dispersion with the photon energy and correspond to the outer $(1b_1, 3a_1, 1b_2)$ and inner $(2a_1)$ valence photoelectrons of $H_2O$ with a possible contribution from the valence lines of $H_2O^+$ and the single-core-ionized $H_2O^+(K^{-1})$ ion. The latter leads to identical final states as produced by the participator HS Auger decay from $K^{-2}V$ states. The outer-valence line was used to calibrate the electron kinetic energy.

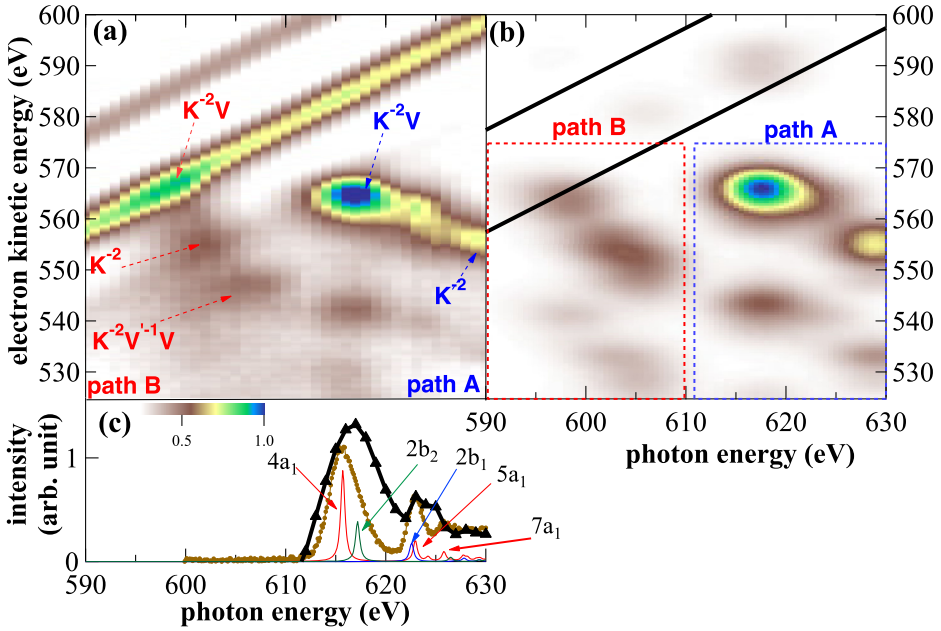


FIG. 2. (a) 2D map for water formed by the electron kinetic-energy spectra as a function of photon energy. The structures above $h\nu = 610$ eV are due to the HS decays of the $K^{-2}V$ states produced via pathway A. The island at $h\nu \approx 616$ eV corresponds to excitations to the states $1s^{-2}4a_1$ and $1s^{-2}2b_2$; compare (c). The clear dependence of the HS Auger transitions on the photon energy indicates a selective excitation of the DCH states, which ends by reaching the $K^{-2}$ double ionization threshold at $h\nu = 631.2$ eV. Below $h\nu \approx 610$ eV three more islands are visible and assigned to excitations via pathway B. Note that the island at the lowest photon energies (600 eV) overlaps with the inner-valence line. (b) Calculated electron emission map combining the calculated Auger electron spectra and the photoionization shake-up and photoexcitation probabilities. The black lines show the valence photoelectron lines considering the valence binding energies of 12.60 and 32.62 eV [35]. (c) The experimental sequential two-photon photoabsorption spectrum produced via pathway A (black triangles) in comparison with the photoelectron shake-up spectrum measured at 2.3 keV (brown dots) [36], which is shifted by the O $1s$ binding energy of 539.8 eV to lower energies. The theoretical results from Ref. [36] simulating the shake-up processes to the $K^{-2}V$ states are also shown.

The calculated electron emission map [Fig. 2(b)], combining the calculated Auger electron spectra using the electronic structure toolkit XMOLECULE [37,38] and the photoionization shake-up and photoexcitation probabilities, reproduces all the observed features on the experimental 2D map. Further details of both calculations can be found in this work and the Supplemental Material [14], enabling a detailed interpretation of these features. The structures observed between photon energies of 610–630 eV and electron kinetic energies of 530–575 eV are attributed to the HS Auger decays of the DCH states generated via pathway A. The resonant islands ($h\nu = 616$–$626$ eV) correspond to the $K^{-2}V$ configurations. The clear dependence on photon energy indicates the selective excitation of the DCH states, starting with $K^{-2}V$ and progressing to the $K^{-2}$ configuration at higher photon energies. These assignments are in excellent agreement with the HS Auger spectrum, which was experimentally and theoretically investigated using a synchrotron radiation source [39]. With the accessible photon intensity at the synchrotron radiation source, the DCH states are formed only through nonselective one-photon processes.

The black triangles in Fig. 2(c) represent the experimental sequential two-photon photoabsorption spectrum in the energy region expected to be dominated by two-photon photoabsorption following path A, i.e., g.s. $\rightarrow$ $K^{-1} \rightarrow K^{-2}V$. It was obtained by integrating the 2D map along the kinetic-energy axis as explained in the Supplemental Material [14]. We also show the O $K^{-2}V$ photoelectron spectrum of water measured at $h\nu = 2.3$ keV (brown dots) which is taken from literature [36]. For comparison, the photoelectron spectrum is shifted to lower energies by 539.8 eV [34], i.e., by the O $1s$ binding energy of $H_2O$, to account for the different initial states of the two experimental spectra. Finally, the red and green lines indicate the calculated spectrum of the photoelectron satellites. A comparison of the experimental spectra shows that the main peak at ≈616 eV, which is assigned to the states $1s^{-2}4a_1$ and $1s^{-2}2b_2$, is clearly blueshifted in the two-photon spectrum (black triangles) as compared to the one-photon photoelectron spectrum (brown dots). This finding can be explained by the fact that in the present two-photon spectrum the transition to the state $1s^{-2}2b_2$ has a higher relative intensity than in the one-photon spectrum; see also our calculations presented in Fig. 3. This is due to the fact that the direct (monopolar) $1s^{-2}4a_1$ channel, present in the one-photon spectrum, is quenched during the two-photon

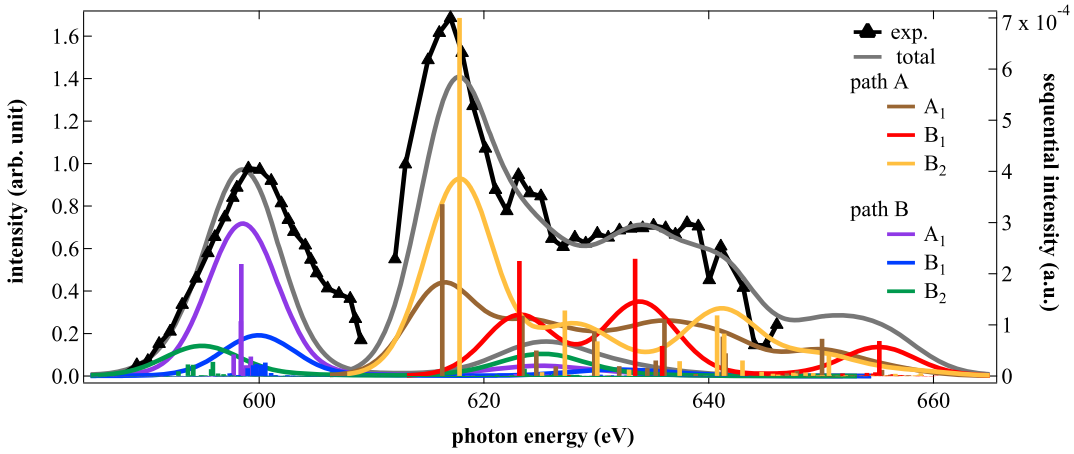


FIG. 3. Right axis: total intensities and excitation energies for all transitions to $K^{-2}V$ states computed with the NOTA + CIPSI strategy. The different vertical colored lines indicate the three final-state symmetries $A_1$, $B_1$, and $B_2$ for both pathway A and B. Left axis: experimental partial electron yield (black triangles) and theoretical photoabsorption (gray line) spectra for the sequential two-photon process via pathway A and B. The different colors indicate the contribution of transitions to $K^{-2}V$ states with $A_1$, $B_1$, and $B_2$ symmetry.

process leaving only the dipolar (or equivalently conjugate) path available. Consequently, the dipolar contribution of $1s^{-2}2b_2$ exceeds that of $1s^{-2}4a1$, as reported in [40].

The structures observed at lower photon energies $h\nu <$ 610 eV are created following path B, i.e., starting from a satellite state created in the first ionization step. The leftmost structure (around 600 eV) is superimposed to the valence line. An easy way to identify these structures is to use the corresponding HS Auger transitions, which are also observed on pathway A. This can be justified by the fact that the intermediate states ($K^{-2}V$ or $K^{-2}$) formed on either path A or B are largely identical, despite a possible small difference due to nuclear dynamics occurring during the lifetime of the intermediate state. Consequently, the island at $h\nu = 600$ eV can be assigned mainly to the decay of the $K^{-2}V$ states $1s^{-2}a_1$ and $1s^{-2}\,2b_2$. The island at $h\nu = 603$ eV can be assigned to the decay of the dicationic $K^{-2}$ state. For the third island at $h\nu = 606$ eV, the situation becomes more complicated since there is no counterpart in the excitation region via path A. Our calculations allow us to presumably attribute this island to the Auger decay of $K^{-2}V'^{-1}V$ states.

Despite the low relative cross section of the shake-up satellite compared to the O 1$s$ main line (about $10^{-2}$) [34], the intensities of the HS Auger electron spectra obtained via either path A or B are almost the same as it can be seen by comparing the intensities (colors) on the 2D map (Fig. 2). As shown in our calculations, these similar intensities are explained by a high cross section for the first step (direct ionization) and a low cross section for the second step (excitation to an unoccupied orbital) of path A as well as the opposite behavior for path B with a low cross section for the shake-up process in the first step and a much higher cross section for the second step.

The calculations are based on the generalization of nonorthogonal transition amplitudes (NOTA) with configuration interaction using perturbative selection made iteratively (CIPSI) wave functions, referred to as NOTA + CIPSI [41]. The method and the intermediate results are presented in the Supplemental Material [14]. These calculations show that the second step is largely dominated by transitions belonging to pathway B, while the probability of formation of intermediate $K^{-1}\,V'^{-1}V$ states is much lower than for the $K^{-1}$ state in the first step. Nuclear dynamics during the sequential core-ionization processes and the subsequent Auger decays are not considered in the calculations. They may have significant impact on the resulting Auger spectrum, but for the identification of the respective structures these details can be neglected.

The total intensities of all sequential two-photon transitions are shown in Fig. 3. Considering the sequential process in its entirety, the relative intensity of both pathway A and pathway B turns out to be of the same order of magnitude, with the intensity of pathway A being slightly higher. To compare our theoretical results with the excitation spectra for pathways A and B extracted from the 2D map, the line spectrum shown in Fig. 3 was convoluted with a Lorentzian function of 0.44 eV FWHM to account for the O $1s^{-2}$ lifetime [42] and a Gaussian function of 7.0 eV FWHM to simulate the experimental photon-energy resolution. The resulting spectra for pathways A and B are shown as gray line in Fig. 3. The subspectra show the contributions of transitions to $K^{-2}V$ final states with $A_1$, $B_1$, and $B_2$ symmetry.

The excellent agreement between the theoretical and experimental spectra allows us to unambiguously identify the origin of the experimentally observed absorption signal in the photon-energy range of 615–645 eV and the

resonance at about 600 eV. The spectral features at higher photon energies are assigned in large majority to the transitions involving the $K^{-1}$ ground state as the intermediate state in the two-photon sequential process. The features at lower photon energies are a clear signature of transitions involving $K^{-1}V'^{-1}V$ excited shake-up states. One can also observe that this pathway yields a small but non-negligible signal in the higher photon-energy region, which is dominated by the pathway A. This small intensity in pathway B is mainly due to the large number of transitions with small intensities. We note that for pathway B, for the photon energy of 606 eV, contributions in the calculated data are significantly lower. We suspect that these are due to multiple shake-up transitions that have not been considered in our theoretical analysis.

A $K^{-2}$ state can be produced resonantly in the same way as for the pathway B but with the difference that the photoionization of the first core electron is accompanied by a shakeoff (instead of a shake-up) of a valence electron. There is also a pathway involving the absorption of three photons: ionization of one valence electron, ionization of the first core electron, and subsequent excitation of the second core electron either into the valence orbital, just emptied by the valence ionization, to produce $K^{-2}$ states or into a higher vacant orbital to produce $K^{-2}V'^{-1}V''^{1}$ states: $V'^{-1} \rightarrow K^{-1}V'^{-1} \rightarrow K^{-2}$ or $K^{-2}V'^{-1}V''$, with $V' = 3a_1, 1b_1, 1b_2$ and $V'' = 4a_1, 5a_1, 2b_1, 2b_2$. A similar valence-ionization core-excitation scheme has been observed for SCH excitations [43,44].

The $K^{-2}V'^{-1}V$ states can be populated either by the three-photon absorption process previously mentioned or by two-photon absorption with a double shake process (shake-up and shakeoff), with up to 30% of the total shake probability [45], followed by photoexcitation ($K^{-1}V^{-1}V'^{-1}V'' \rightarrow K^{-2}V'^{-1}V''$ or $K^{-2}V^{-1}V''$ with $V'' = 4a_1, 5a_1, 2b_1, 2b_2$). It is worth noting that the $K^{-2}V$ states cannot be produced following this three-photon process with one-color photon beam, as it involves passing through two distinct excitation transitions.

In summary, we have studied experimentally and theoretically the formation of $K^{-2}V$ states in isolated water molecules by the sequential absorption of two x-ray photons. The present study reveals a second important pathway for the population of DCH states, which has comparable probability but occurs at a lower photon energy as compared to the pathway (A) $K^{-1} \rightarrow K^{-2}V$. In this pathway, the first step of core ionization is accompanied by the shake-up of a valence electron. This is followed by the promotion of the second core electron into the newly vacant orbital ($K^{-1}V'^{-1}V \rightarrow K^{-2}V$). While the cross section for the first step of this pathway is small, the increased overlap of the valence hole with the core electron leads to a drastic increase in the cross section for the second step. Identifying these two distinct pathways to the same final states is nontrivial, and it was made possible by exploiting simultaneously the main characteristics of the x-ray source, namely its high intensity, delivery of very short pulses, and full tunability.

We believe that the role played by the shake-up processes, which may be intuitively underestimated, is important in the resonant selective production of DCH states. The revealed alternative pathway holds great importance in enhancing our understanding of the absorption of multiple photons in the interaction between light and matter, especially under extreme conditions. Furthermore, the general aspect of shake-up processes implies that the alternative pathway should be taken into account not only in gas but also in liquid and solid phases.

The experimental data were collected during user beam time 2620. The metadata are available at [46].

We acknowledge European XFEL in Schenefeld, Germany, for the provision of XFEL beam time at the SQS instrument and would like to thank the staff for their assistance. The authors would like to thank Alexei Grum-Grzhimailo and Ekaterina Voronina for fruitful discussions. A. F., R. T., and S. C. thank Labex MiChem part of French state funds managed by the ANR within the Investissements d'Avenir programme (Sorbonne Université, ANR-11-IDEX-0004-02), for providing A. F.'s Ph.D. funding. D. P., A. V., J. D. B., and M. S. acknowledge the financial support of the CNRS GotoXFEL program. N. V. and T. M. acknowledges funding from the European Union's Horizon 2020 research and innovation programme under the Marie Skłodowska-Curie Grant Agreement No. 860553. F. T. acknowledges support by the MaxWater initiative of the Max-Planck-Gesellschaft. D. K. also acknowledges support from the U.S. Department of Energy, Office of Basic Energy Sciences, Division of Chemical Sciences, Geosciences and Biosciences through Argonne National Laboratory. M. M. acknowledges support by the DFG, German Research Foundation–SFB-925–Project No. 170620586. M. M. and L. I. acknowledge support from the Cluster of Excellence "CUI: Advanced Imaging of Matter" of the Deutsche Forschungsgemeinschaft (DFG)—EXC 2056—Project ID 390715994. G. S. acknowledges financial support from the Deutsche Forschungsgemeinschaft Research Training Group DynCAM (RTG 2717) and Grant No. 429805582 (Project No. SA 3470/4-1). L. I. acknowledges support from DESY (Hamburg, Germany), a member of the Helmholtz Association HGF. Work by K. L., G. D. and L. Y. Work by J. R. R. was supported by the U.S. Department of Energy, Office of Science, Basic Energy Science, Chemical Sciences, Geosciences and Biosciences Division under Contract No. DE-AC02-06CH11357.

*iyas.ismail@sorbonne-universite.fr
†marc.simon@sorbonne-universite.fr

[1] N. Berrah, L. Fang, B. Murphy, T. Osipov, K. Ueda, E. Kukk, R. Feifel, P. van der Meulen, P. Salen, H. T. Schmidt *et al.*, Double-core-hole spectroscopy for chemical analysis with an intense x-ray femtosecond laser, Proc. Natl. Acad. Sci. U.S.A. **108**, 16912 (2011).

[2] P. Salén, P. van der Meulen, H. T. Schmidt, R. D. Thomas, M. Larsson, R. Feifel, M. N. Piancastelli, L. Fang, B. Murphy, T. Osipov, N. Berrah, E. Kukk, K. Ueda, J. D. Bozek, C. Bostedt, S. Wada, R. Richter, V. Feyer, and K. C. Prince, Experimental verification of the chemical sensitivity of two-site double core-hole states formed by an x-ray free-electron laser, Phys. Rev. Lett. **108**, 153003 (2012).

[3] T. Mazza *et al.*, Mapping resonance structures in transient core-ionized atoms, Phys. Rev. X **10**, 041056 (2020).

[4] L. Inhester, G. Groenhof, and H. Grubmüller, Core hole screening and decay rates of double core ionized first row hydrides, J. Chem. Phys. **138**, 164304 (2013).

[5] G. Goldsztejn, T. Marchenko, R. Püttner, L. Journel, R. Guillemin, S. Carniato, P. Selles, O. Travnikova, D. Céolin, A. F. Lago, R. Feifel, P. Lablanquie, M. N. Piancastelli, F. Penent, and M. Simon, Double-core-hole states in neon: Lifetime, post-collision interaction, and spectral assignment, Phys. Rev. Lett. **117**, 133001 (2016).

[6] M. Žitnik, R. Püttner, G. Goldsztejn, K. Bučar, M. Kavčič, A. Mihelič, T. Marchenko, R. Guillemin, L. Journel, O. Travnikova *et al.*, Two-to-one Auger decay of a double L vacancy in argon, Phys. Rev. A **93**, 021401(R) (2016).

[7] T. Jahnke *et al.*, Inner-shell-ionization-induced femtosecond structural dynamics of water molecules imaged at an x-ray free-electron laser, Phys. Rev. X **11**, 041044 (2021).

[8] L. S. Cederbaum, F. Tarantelli, A. Sgamellotti, and J. Schirmer, On double vacancies in the core, J. Chem. Phys. **85**, 6513 (1986).

[9] R. Santra, N. V. Kryzhevoi, and L. S. Cederbaum, X-ray two-photon photoelectron spectroscopy: A theoretical study of inner-shell spectra of the organic para-aminophenol molecule, Phys. Rev. Lett. **103**, 013002 (2009).

[10] D. Koulentianos, S. Carniato, R. Püttner, G. Goldsztejn, T. Marchenko, O. Travnikova, L. Journel, R. Guillemin, D. Céolin, M. L. M. Rocco, M. N. Piancastelli, R. Feifel, and M. Simon, Double-core-hole states in $CH_3CN$: Pre-edge structures and chemical-shift contributions, J. Chem. Phys. **149**, 134313 (2018).

[11] L. Young, E. P. Kanter, B. Krässig, Y. Li, A. M. March, S. T. Pratt, R. Santra, S. H. Southworth, N. Rohringer, L. F. DiMauro *et al.*, Femtosecond electronic response of atoms to ultra-intense x-rays, Nature (London) **466**, 56 (2010).

[12] M. Hoener *et al.*, Ultraintense x-ray induced ionization, dissociation, and frustrated absorption in molecular nitrogen, Phys. Rev. Lett. **104**, 253002 (2010).

[13] J. Miao, T. Ishikawa, I. K. Robinson, and M. M. Murnane, Beyond crystallography: Diffractive imaging using coherent x-ray light sources, Science **348**, 530 (2015).

[14] See Supplemental Material at http://link.aps.org/supplemental/10.1103/PhysRevLett.131.253201 for additional details of the calculations and the experiment, which includes Refs. [15–33].

[15] T. Mazza, T. M. Baumann, R. Boll, A. De Fanis, P. Grychtol, M. Ilchen, J. Montaño, V. Music, Y. Ovcharenko, N. Rennhack *et al.*, The beam transport system for the Small Quantum Systems instrument at the European XFEL: Optical layout and first commissioning results, J. Synchrotron Radiat. **30**, 457 (2023).

[16] W. Decking *et al.*, A MHz-repetition-rate hard x-ray free-electron laser driven by a superconducting linear accelerator, Nat. Photonics **14**, 391 (2020).

[17] T. Tschentscher, C. Bressler, J. Grünert, A. Madsen, A. P. Mancuso, M. Meyer, A. Scherz, H. Sinn, and U. Zastrau, Photon beam transport and scientific instruments at the European XFEL, Appl. Sci. **7**, 592 (2017).

[18] A. De Fanis, M. Ilchen, A. Achner, T. M. Baumann, R. Boll, J. Buck, D. Danilevsky, C. Esenov, B. Erk, P. Grychtol *et al.*, High-resolution electron time-of-flight spectrometers for angle-resolved measurements at the SQS instrument at the European XFEL, J. Synchrotron Radiat. **29**, 755 (2022).

[19] A. Ferté, F. Penent, J. Palaudoux, H. Iwayama, E. Shigemasa, Y. Hikosaka, K. Soejima, P. Lablanquie, R. Taïeb, and S. Carniato, Specific chemical bond relaxation unraveled by analysis of shake-up satellites in the oxygen single site double core hole spectrum of $CO_2$, Phys. Chem. Chem. Phys. **24**, 1131 (2022).

[20] Y. Garniron, T. Applencourt, K. Gasperich, A. Benali, A. Ferté, J. Paquier, B. Pradines, R. Assaraf, P. Reinhardt, J. Toulouse, P. Barbaresco, N. Renon, G. David, J.-P. Malrieu, M. Véril, M. Caffarel, P.-F. Loos, E. Giner, and A. Scemama, QUANTUM PACKAGE 2.0: An open-source determinant-driven suite of programs, J. Chem. Theory Comput. **15**, 3591 (2019).

[21] R. L. Martin and D. A. Shirley, Theory of core-level photoemission correlation state spectra, J. Chem. Phys. **64**, 3685 (1976).

[22] M. Nakano, P. Selles, P. Lablanquie, Y. Hikosaka, F. Penent, E. Shigemasa, K. Ito, and S. Carniato, Near-edge x-ray absorption fine structures revealed in core ionization photoelectron spectroscopy, Phys. Rev. Lett. **111**, 123001 (2013).

[23] S. Carniato, P. Selles, A. Ferté, N. Berrah, A. Wuosmaa, M. Nakano, Y. Hikosaka, K. Ito, M. Žitnik, K. Bučar *et al.*, Single photon simultaneous K-shell ionization/excitation in $C_6H_6$: Experiment and theory, J. Phys. B **53**, 244010 (2020).

[24] P. S. Bagus, Self-consistent-field wave functions for hole states of some Ne-like and Ar-like ions, Phys. Rev. **139**, A619 (1965).

[25] A. T. B. Gilbert, N. A. Besley, and P. M. W. Gill, Self-consistent field calculations of excited states using the maximum overlap method (MOM), J. Phys. Chem. A **112**, 13164 (2008).

[26] P. S. Bagus and H. F. Schaefer, III, Direct near-Hartree–Fock calculations on the 1s hole states of $NO^+$, J. Chem. Phys. **55**, 1474 (1971).

[27] M. H. Wood, On the calculation of the satellite peaks observed in the high energy photoelectron spectra of small molecules, Chem. Phys. **5**, 471 (1974).

[28] L. S. Cederbaum, W. Domcke, and J. Schirmer, Many-body theory of core holes, Phys. Rev. A **22**, 206 (1980).

[29] L. S. Cederbaum, Many-body theory of multiple core holes, Phys. Rev. A **35**, 622 (1987).

[30] T. H. Dunning, Jr., Gaussian basis sets for use in correlated molecular calculations. I. The atoms boron through neon and hydrogen, J. Chem. Phys. **90**, 1007 (1989).

[31] R. A. Kendall, T. H. Dunning, and R. J. Harrison, Electron affinities of the first-row atoms revisited. Systematic basis sets and wave functions, J. Chem. Phys. **96**, 6796 (1992).
[32] H. Ågren, S. Svensson, and U. I. Wahlgren, SCF and limited CI calculations for assignment of the Auger spectrum and of the satellites in the soft x-ray spectrum of $H_2O$, Chem. Phys. Lett. **35**, 336 (1975).
[33] H. Siegbahn, L. Asplund, and P. Kelfve, The Auger electron spectrum of water vapour, Chem. Phys. Lett. **35**, 330 (1975).
[34] R. Sankari, M. Ehara, H. Nakatsuji, A. De Fanis, H. Aksela, S. L. Sorensen, M. N. Piancastelli, E. Kukk, and K. Ueda, High resolution O 1s photoelectron shake-up satellite spectrum of $H_2O$, Chem. Phys. Lett. **422**, 51 (2006).
[35] B. Winter, R. Weber, W. Widdra, M. Dittmar, M. Faubel, and I. V. Hertel, Full valence band photoemission from liquid water using EUV synchrotron radiation, J. Phys. Chem. A **108**, 2625 (2004).
[36] T. Marchenko, S. Carniato, G. Goldsztejn, O. Travnikova, L. Journel, R. Guillemin, I. Ismail, D. Koulentianos, J. Martins, D. Céolin, R. Püttner, M. N. Piancastelli, and M. Simon, Single and multiple excitations in double-core-hole states of free water molecules, J. Phys. B **53**, 224002 (2020).
[37] Y. Hao, L. Inhester, K. Hanasaki, S.-K. Son, and R. Santra, Efficient electronic structure calculation for molecular ionization dynamics at high x-ray intensity, Struct. Dyn. **2**, 041707 (2015).
[38] L. Inhester, K. Hanasaki, Y. Hao, S.-K. Son, and R. Santra, X-ray multiphoton ionization dynamics of a water molecule irradiated by an x-ray free-electron laser pulse, Phys. Rev. A **94**, 023422 (2016).
[39] T. Marchenko, L. Inhester, G. Goldsztejn, O. Travnikova, L. Journel, R. Guillemin, I. Ismail, D. Koulentianos, D. Céolin, R. Püttner, M. N. Piancastelli, and M. Simon, Ultrafast nuclear dynamics in the doubly-core-ionized water molecule observed via Auger spectroscopy, Phys. Rev. A **98**, 063403 (2018).
[40] S. Carniato, P. Selles, L. Andric, J. Palaudoux, F. Penent, M. Žitnik, K. Bučar, M. Nakano, Y. Hikosaka, K. Ito, and P. Lablanquie, Single photon simultaneous K-shell ionization and K-shell excitation. I. Theoretical model applied to the interpretation of experimental results on $H_2O$, J. Chem. Phys. **142**, 014307 (2015).
[41] A. Ferté, J. Palaudoux, F. Penent, H. Iwayama, E. Shigemasa, Y. Hikosaka, K. Soejima, K. Ito, P. Lablanquie, R. Taïeb, and S. Carniato, Advanced computation method for double core hole spectra: Insight into the nature of intense shake-up satellites, J. Phys. Chem. Lett. **11**, 4359 (2020).
[42] L. Inhester, G. Groenhof, and H. Grubmüller, Core hole screening and decay rates of double core ionized first row hydrides, J. Chem. Phys. **138**, 164304 (2013).
[43] E. P. Kanter, B. Krässig, Y. Li, A. M. March, P. Ho, N. Rohringer, R. Santra, S. H. Southworth, L. F. DiMauro, G. Doumy *et al.*, Unveiling and driving hidden resonances with high-fluence, high-intensity x-ray pulses, Phys. Rev. Lett. **107**, 233001 (2011).
[44] Z.-H. Loh, G. Doumy, C. Arnold, L. Kjellsson, S. H. Southworth, A. Al Haddad, Y. Kumagai, M.-F. Tu, P. J. Ho, A. M. March *et al.*, Observation of the fastest chemical processes in the radiolysis of water, Science **367**, 179 (2020).
[45] A. G. Kochur and V. A. Popov, Probabilities of multiple shake processes in sudden approximation, J. Phys. B **39**, 3335 (2006).
[46] 10.22003/XFEL.EU-DATA-002620-00.